



**HAL**  
open science

## Observations of near-surface carbon monoxide from space using MOPITT multispectral retrievals

H.M. Worden, M. N. Deeter, D.P. Edwards, J.C. Gille, J.R. Drummond, P. Nédélec

► **To cite this version:**

H.M. Worden, M. N. Deeter, D.P. Edwards, J.C. Gille, J.R. Drummond, et al.. Observations of near-surface carbon monoxide from space using MOPITT multispectral retrievals. *Journal of Geophysical Research: Atmospheres*, 2010, 115, pp.D18314. 10.1029/2010JD014242 . hal-00563703

**HAL Id: hal-00563703**

**<https://hal.science/hal-00563703>**

Submitted on 23 Jun 2022

**HAL** is a multi-disciplinary open access archive for the deposit and dissemination of scientific research documents, whether they are published or not. The documents may come from teaching and research institutions in France or abroad, or from public or private research centers.

L'archive ouverte pluridisciplinaire **HAL**, est destinée au dépôt et à la diffusion de documents scientifiques de niveau recherche, publiés ou non, émanant des établissements d'enseignement et de recherche français ou étrangers, des laboratoires publics ou privés.

Copyright

## Observations of near-surface carbon monoxide from space using MOPITT multispectral retrievals

H. M. Worden,<sup>1</sup> M. N. Deeter,<sup>1</sup> D. P. Edwards,<sup>1</sup> J. C. Gille,<sup>1</sup> J. R. Drummond,<sup>2</sup> and P. Nédélec<sup>3</sup>

Received 19 March 2010; revised 24 May 2010; accepted 28 May 2010; published 28 September 2010.

[1] Using both thermal infrared (TIR) and near infrared (NIR) channels of MOPITT (Measurements of Pollution in the Troposphere) on EOS-Terra, we demonstrate the first coincident multispectral retrievals of carbon monoxide (CO) from space. Exploiting both TIR and NIR channels has been possible due to recent progress in characterizing NIR channel radiance errors. This has allowed us to trade off sensitivity to near surface CO for larger random errors in the combined retrieval. By examining retrieval diagnostics such as DFS (degrees of freedom for signal) and averaging kernels for the multispectral retrieval (TIR + NIR) as compared to the TIR-only retrieval, we find that adding the NIR channel to the retrieval significantly increases sensitivity to CO, especially near the surface, but with high spatial variability due to surface albedo variations. The cases with the largest increases in DFS are over regions with low thermal contrast between the surface and lower atmosphere. In the tropics (23.4°S–23.4°N), the fraction of daytime land cases with at least 0.4 DFS in the surface layer (surface to 800 hPa) is 20% for TIR-only retrievals compared to 59% for multispectral retrievals. Vertical resolution for the surface layer is also improved, in some cases from around 6 km for TIR-only to roughly 1 km for TIR + NIR. Since we apply a single a priori CO profile (unlike MOPITT V4) and error covariance in all the retrievals reported here, these increases are due solely to the addition of the NIR channel. Enhanced sensitivity to near surface CO is especially evident in a case study for central/east Asia where source regions for urban areas with high population density are clearly identifiable. Although these retrievals are still a research product and require further validation and scientific evaluation, they demonstrate the increased sensitivity to CO in the lowermost troposphere that can be obtained from multispectral MOPITT data.

**Citation:** Worden, H. M., M. N. Deeter, D. P. Edwards, J. C. Gille, J. R. Drummond, and P. Nédélec (2010), Observations of near-surface carbon monoxide from space using MOPITT multispectral retrievals, *J. Geophys. Res.*, *115*, D18314, doi:10.1029/2010JD014242.

### 1. Introduction

[2] Observations of tropospheric carbon monoxide (CO) from space over the last decade have greatly advanced the understanding of atmospheric composition and dynamics and the capability to model processes from global pollution transport [e.g., *Turquety et al.*, 2008; *Edwards et al.*, 2006] to continental scale source emissions [e.g., *Arellano et al.*, 2004; *Pfister et al.*, 2005a; *Jones et al.*, 2009; *Kopacz et al.*, 2010]. Several satellite sensors now measure CO in the troposphere.

MOPITT (Measurement of Pollution in the Troposphere) on EOS-Terra, launched December 1999 [e.g., *Drummond*, 1992; *Deeter et al.*, 2003], AIRS (Atmospheric Infrared Sounder), on EOS-Aqua, launched May 2002 [*Warner et al.*, 2007], TES (Tropospheric Emission Spectrometer), on EOS-Aura, launched July 2004 [*Luo et al.*, 2007], and IASI (Infrared Atmospheric Sounding Interferometer) on METOP-A, launched October 2006 [*George et al.*, 2009], all use thermal infrared (TIR) absorption around 4.7  $\mu\text{m}$  to retrieve vertical profiles of CO abundance. MOPITT and SCIAMACHY (Scanning Imaging Absorption Spectrometer for Atmospheric Cartography, on Envisat), launched March 2002 [*Buchwitz et al.*, 2004], both use solar reflection in the near-infrared (NIR) with CO absorption around 2.3  $\mu\text{m}$  to retrieve a CO column abundance.

[3] Current operational remote sensing measurements of CO are typically most sensitive to the middle troposphere for TIR measurements [*Deeter et al.*, 2004; *Warner et al.*, 2007; *Luo et al.*, 2007; *George et al.*, 2009] and to a total

<sup>1</sup>Atmospheric Chemistry Division, National Center for Atmospheric Research, Boulder, Colorado, USA.

<sup>2</sup>Department of Physics and Atmospheric Science, Dalhousie University, Halifax, Nova Scotia, Canada.

<sup>3</sup>Laboratoire d'Aérodynamique, Université P. Sabatier, Centre National de la Recherche Scientifique, Observatoire Midi-Pyrénées, Toulouse, France.

column for NIR measurements [Deeter et al., 2009; Buchwitz et al., 2004, 2007]. Under conditions with good thermal contrast (usually found in arid regions), sensitivity close to the surface is obtainable with TIR measurements [Deeter et al., 2007a; Clerbaux et al., 2008]. Turquety et al. [2008] combined postretrieval MOPITT CO profiles and SCIAMACHY column CO to infer boundary layer residual CO but showed that measurement errors and instrument inconsistencies precluded a quantitative result. As we will demonstrate, combining the TIR and NIR measurements in a common retrieval allows a significant increase in sensitivity to CO in the lowermost troposphere.

[4] Retrieval sensitivity to the lowermost troposphere is critical for the operational use of satellite data in air quality and climate applications and has motivated previous investigations on the use of multispectral data for measuring CO and other species. Increased sensitivity to near surface CO from the TIR + NIR retrieval was predicted using MOPITT preflight simulations [Pan et al., 1995] and also shown by recent satellite Observation System Simulation Experiment (OSSE) analyses [Edwards et al., 2009]. Using both thermal and near-infrared frequencies should provide sensitivity to near surface CO<sub>2</sub> [Christi and Stephens, 2004] and preliminary results from IASI [Razavi et al., 2009] for multispectral retrievals of methane using bands at 7.7 and 3.7  $\mu\text{m}$  have suggested enhanced sensitivity to near surface concentrations. Similar behavior has also been predicted for multispectral retrievals of ozone profiles from simulated TIR and ultraviolet (UV) radiances [Worden et al., 2007; Landgraf and Hasekamp, 2007]. Both of these studies found increased sensitivity in the averaging kernel (AK) near the surface when combining radiances that provide column information (UV measurements for the case of ozone) with TIR radiances that provide profile information, especially in cases with small thermal contrast, as we show here for CO.

[5] Because of its relatively long chemical lifetime ( $\sim 2$  months), CO is a very useful tracer for pollution transport, but using presently available satellite CO measurements for inverse modeling or assimilation, transport from the boundary layer to the free troposphere must be inferred from other information such as meteorological data or model fields. With their added information in the lowermost troposphere, these multispectral retrievals have important implications for understanding surface emissions and their subsequent transport to the free troposphere.

[6] This paper is organized as follows. Section 2 describes the MOPITT TIR and NIR measurements and retrieval methodology using the existing MOPITT algorithms for optimal estimation. Section 2 also discusses the characterization of NIR geophysical noise and shows examples of the resulting vertical sensitivity (averaging kernel) for a multispectral retrieval. Section 3 presents global maps of seasonal averages from the combined TIR and NIR retrievals (TIR + NIR) as compared to retrievals from TIR channels only (TIR only). Section 4 gives a case study over China as an example of the increase in information for surface CO from the TIR + NIR retrievals, and section 5 gives conclusions and our plans for future work and new

MOPITT data products. A list of acronyms is provided after section 5.

## 2. MOPITT Measurements and CO Retrievals

### 2.1. Measurements

[7] MOPITT is a multichannel instrument that uses correlation radiometry [Drummond, 1992; Tolton and Drummond, 1997; Edwards et al., 1999; Drummond et al., 2009] to detect atmospheric CO absorption at 4.7  $\mu\text{m}$  (TIR channels) and 2.3  $\mu\text{m}$  (NIR channels). The transmission through gas cells containing CO is modulated by varying gas cell pressure or path length, with gas cells designated as PMC (pressure modulated cell) or LMC (length modulated cell). Modulations in the gas cell change the observed radiance only near the spectral positions of CO lines. Since the widths of absorption lines vary with cell length or pressure, TOA (top of atmosphere) radiances measured by different cells have sensitivity to the pressure broadened absorption of CO at different altitudes in the atmosphere. TIR channels 1 and 5 incorporate LMCs; TIR channels 3 and 7 incorporate PMCs and NIR channels 2 and 6 both incorporate LMCs. (Methane channels 4 and 8 are not discussed here [see Pfister et al., 2005b]). In this paper, we are considering data from 2004 to 2008, which were taken after the loss of MOPITT channels 1–4 in May 2001 [Deeter et al., 2004], i.e., only channels 5, 6, and 7 are utilized here.

[8] Using the radiances transmitted through the cells for low and high absorption, we compute average ( $A$ ) signals for the mean radiance and difference ( $D$ ) signals for low-high cell absorption radiances. For TIR signals, the  $A$  signals provide more information about surface temperature and emissivity, while  $D$  signals respond more to differences in the atmospheric profile of CO [Edwards et al., 1999]. For NIR measurements, we use the radiance ratio  $R = D/A$  to estimate CO column abundance [Deeter et al., 2009]. To first-order approximation, this allows the cancellation of surface reflectance in the NIR retrieval, since CO absorption lines have a nearly uniform spectral distribution and the spectral dependence of reflectivity across the relatively narrow filter band pass ( $\sim 2.32$ – $2.35 \mu\text{m}$ ) is spectrally flat in most cases [Pfister et al., 2005b]. For the combined TIR and NIR retrievals, we use radiances  $5A$ ,  $5D$ , and  $7D$  for TIR and radiance ratios  $6R = 6D/6A$  for NIR. Corresponding instrument noise estimates are computed from calibration measurements for the cold-space view.

[9] Since the NIR signals depend on reflected solar radiance from the surface [Deeter et al., 2009], we can only use daytime land observations, taken around 10:30 am local time, for these combined retrievals. (Although some ocean solar reflection occurs under “Sun-glint” conditions, polarization effects would have to be characterized for this to be a reliable source of NIR signal for MOPITT, as discussed by Pfister et al. [2005b]). We also use only cloud-free scenes, applying the same cloud screening approach used for standard MOPITT data processing, which combines the MODIS (Moderate-Resolution Imaging Spectroradiometer) cloud mask [Ackerman et al., 1998] with MOPITT cloud detection [Warner et al., 2001].

## 2.2. Optimal Estimation Retrievals

[10] The combined TIR and NIR retrievals use the existing MOPITT forward model [Edwards *et al.*, 1999] and retrieval [Pan *et al.*, 1998; Deeter *et al.*, 2003, 2009, 2010] algorithms, with the same assumptions for parameters such as atmospheric temperature and water vapor and their related errors. The forward model produces synthetic  $A$ ,  $D$ , and  $R$  signals for a given atmospheric state, along with weighting functions  $\mathbf{K}$ , which are then inverted in a maximum a posteriori (MAP) solution, following Rodgers [2000], to update the estimated state vector,

$$\hat{\mathbf{x}} = \mathbf{x}_a + \mathbf{S}_a \mathbf{K}^T (\mathbf{K} \mathbf{S}_a \mathbf{K}^T + \mathbf{S}_e)^{-1} (\mathbf{y} - \mathbf{K} \mathbf{x}_a), \quad (1)$$

where  $\mathbf{x}_a$  is the a priori state vector,  $\mathbf{S}_a$  is the a priori error covariance,  $\mathbf{S}_e$  is the measurement error covariance, and  $\mathbf{y}$  is the measurement vector. Here we use the same retrieval state vector developed for MOPITT V4 processing with CO parameters specified in log VMR (volume mixing ratio) [Deeter *et al.*, 2010].

[11] We can characterize the ability of the retrieval to measure the true state vector  $\mathbf{x}$ , by writing the estimate in terms of a gain matrix  $\mathbf{G}$  and averaging kernel matrix  $\mathbf{A}$ ,

$$\hat{\mathbf{x}} = \mathbf{x}_a + \mathbf{A}(\mathbf{x} - \mathbf{x}_a) + \mathbf{G}\mathbf{e}, \quad (2)$$

where  $\mathbf{e}$  is the measurement error vector,  $\mathbf{G} = (\mathbf{K}^T \mathbf{S}_e^{-1} \mathbf{K} + \mathbf{S}_a^{-1})^{-1} \mathbf{K}^T \mathbf{S}_e^{-1}$  and  $\mathbf{A} = \mathbf{G}\mathbf{K}$ . The averaging kernel (AK) matrix  $\mathbf{A}$  represents the sensitivity of the retrieved parameters to the true state, giving a quantitative measure of the vertical sensitivity and resolution for each retrieval. As evident in equation (2), our estimate at a given pressure level will be close to the true state, within measurement error, when the corresponding row of  $\mathbf{A}$  is close to unity for the diagonal. Likewise, the estimate will be dominated by the a priori profile if the averaging kernel row at that pressure becomes negligible. In this study, we use DFS, computed as the trace of  $\mathbf{A}$ , as well as the surface layer DFS (trace of  $\mathbf{A}$  for the lowest levels), to compare relative measurement sensitivity to CO at different geographic locations.

### 2.2.1. Characterizing MOPITT NIR Errors

[12] In the MOPITT optimal estimation-based retrieval algorithm, expected radiance error statistics are represented by the radiance error covariance matrix  $\mathbf{S}_e$ . This matrix is formed by summing the forward model error covariance matrix  $\mathbf{S}_f$  and the instrument noise covariance matrix  $\mathbf{S}_y$ . Methods for determining  $\mathbf{S}_f$  and  $\mathbf{S}_y$  are described in the work of Deeter *et al.* [2003]. For the work reported here, the geophysical noise term for channel 6 (NIR) is incorporated into the instrument noise covariance matrix  $\mathbf{S}_y$ .

[13] As shown in Deeter *et al.* [2009], the instrumental measurement uncertainty for NIR ratio  $6D/6A$ ,  $\sigma_R$ , can be approximated by,

$$\sigma_R^2 \approx \left( \frac{\sigma_D}{A} \right)^2, \quad (3)$$

where  $\sigma_D$  is the uncertainty in  $D$  measured during calibration. In addition to the instrumental uncertainty, there is an important radiance error contribution due to the changing field of view (FOV) caused by satellite motion during the time taken to make a single measurement. For the MOPITT NIR channel, this ‘‘geophysical noise’’ is generally larger

than the estimated noise from calibration. In the work of Deeter *et al.* [2009], the NIR calibration noise was scaled by a factor of 5 to account for geophysical noise; however, for the multispectral retrievals, this approach allowed only minimal information from the NIR channel to contribute in the combined retrievals (e.g., DFS increases  $< 0.05$ ). For this study, we assume that the geophysical noise for  $6R$ ,  $\sigma_{geo}$ , is added in quadrature to the instrument noise, i.e.,

$$\sigma_R^2 \approx \left( \frac{\sigma_D}{A} \right)^2 + \sigma_{geo}^2. \quad (4)$$

In order to maximize the impact of the NIR observations in the combined retrieval, we select a value for  $\sigma_{geo}$  in equation (4), which is close to the minimum value required to regularize the retrievals and limit the number of nonconvergent cases. The value added for  $\sigma_{geo}$  for the NIR is nearly equivalent to the NIR calibration noise, thereby increasing this noise by a factor  $\sim \sqrt{2}$ . This is less than the factor assumed in the work of Deeter *et al.* [2009], but it allows the information from the NIR observations to propagate into the combined retrievals, as measured by retrieval DFS, at the expense of increased random errors that will be underestimated in the retrieval error covariance. The effects of these random errors can be seen in Figure 1 where we compare single MOPITT TIR + NIR observations of surface CO taken over a week with  $1^\circ \times 1^\circ$  binned averages, with a mean of  $N = 10.7$  observations per bin. Figure 1 also shows that the average estimated surface CO error from the retrieval is often much smaller than the standard deviation for the same latitude/longitude bin, due to underestimated retrieval errors along with actual CO variability. In order to mitigate the effects of random error for this study, we use both spatial and temporal averages to show the persistent features that are observable with multispectral MOPITT retrievals.

[14] Although the added noise term for geophysical error described above is sufficient for multispectral retrievals that demonstrate boundary layer sensitivity, the retrievals would not provide an accurate estimate of the a posteriori error covariance and they do not account for spectral variability of the surface reflectance or aerosol interference. Work to improve the characterization of NIR radiance errors is in progress. For SCIAMACHY column CO measurements ( $2.3 \mu\text{m}$ ), Gloudemans *et al.* [2008], find errors due to aerosols that depend mainly on AOD (aerosol optical depth), aerosol type, and surface albedo. They found that for most albedo types (albedo  $< 0.2$ ), aerosol scattering reduces the effective optical path and results in a smaller retrieved column, with errors around  $\sim 2\%$  for industrial aerosols and up to  $9\%$  for biomass burning and mineral dust aerosols. Over bright surfaces (high albedo), aerosols can enhance the apparent column, with errors up to  $10\%$  for mineral dust aerosols over deserts. Previous studies by the MOPITT team on the effects of fine mode AOD on MOPITT NIR signals found that the gas correlation technique along with the use of a radiance ratio significantly reduces errors due to aerosols with a relatively flat spectral dependence, but this needs further analysis for other aerosol types including dust.

### 2.2.2. A priori

[15] All of the MOPITT retrieval types discussed in this paper use the same global, static a priori vector  $\mathbf{x}_a$  as dis-

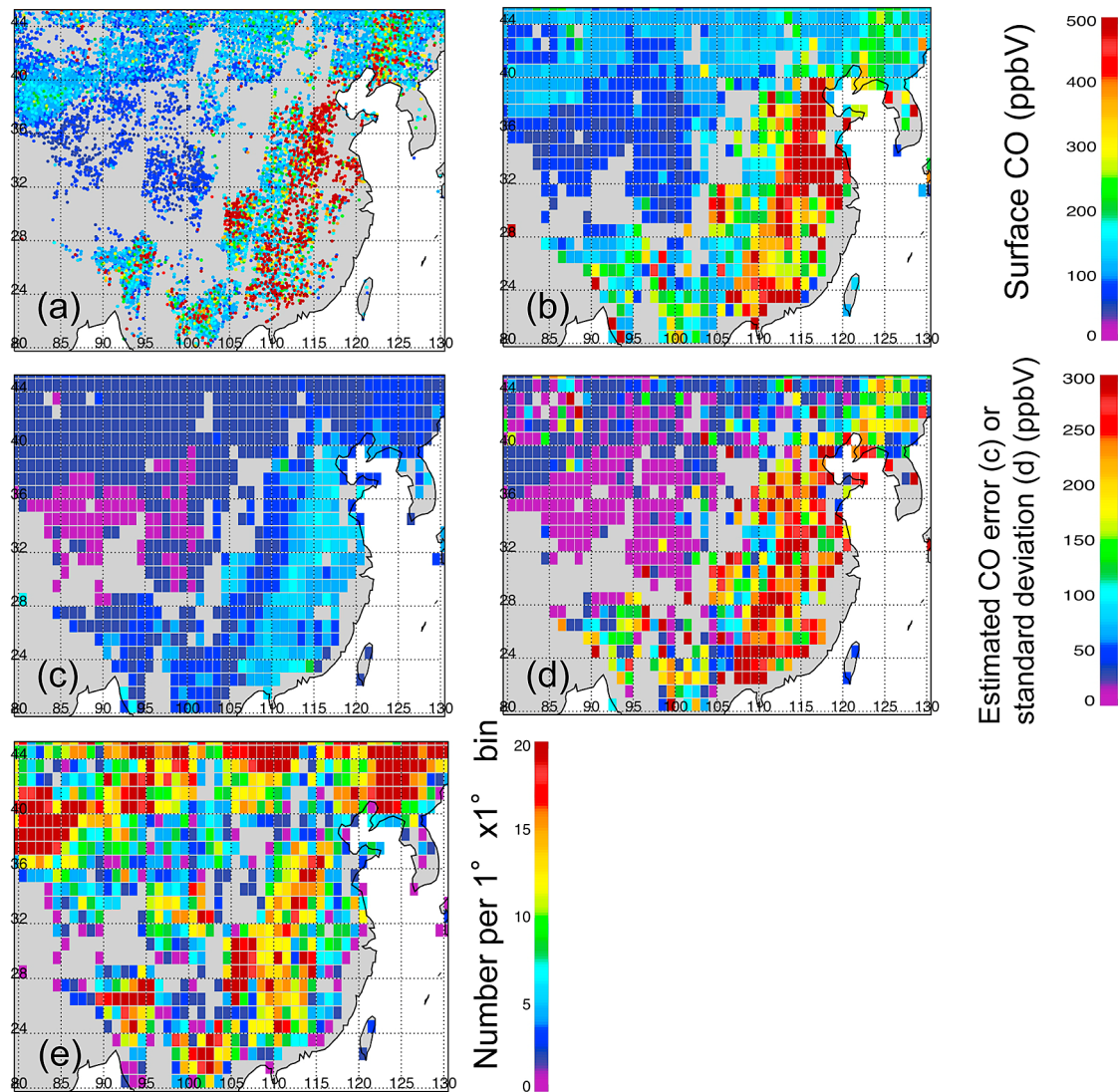


**Figure 1.** Example of MOPITT TIR + NIR Asian observations for 1 week: 9–15 September 2005. (a) Individual retrievals of surface CO. (b) The same retrievals binned by  $1^\circ \times 1^\circ$ . (c) The average surface CO retrieval error. (d) The standard deviation of surface CO in each bin. (e) The number of observations per bin. All panels indicate longitude and latitude in degrees.

tinguished from the spatially and temporally variable a priori based on a CO climatology from the MOZART model used in MOPITT V4 retrievals [Deeter *et al.*, 2010]. The purpose of using a common a priori profile in this new multispectral retrieval is to demonstrate differences from the TIR-only case due to the NIR measurements alone, without having to account for spatial/temporal differences in the a priori as well. The a priori profile assumed for these retrievals is shown in Figures 2d–2f and is the result of applying a lognormal average to the same global distribution of CO profiles used for the MOPITT V3 a priori [Deeter *et al.*, 2007b]. The a priori error covariance  $S_a$  used to constrain the retrievals has the same specification as used for MOPITT V4 data with 30% variance in VMR and a vertical correlation distance specified in pressure coordinates of 100 hPa. Since the reported values of DFS depend on both measurement signal-to-noise and retrieval specifica-

tions, our choice of a priori covariance affects the values of DFS, making absolute values somewhat difficult to compare with retrievals for other instruments. However, for this study, the relative increase in DFS from TIR-only to TIR-NIR retrievals is significant since the same a priori covariance is applied in both.

### 2.3. Vertical Sensitivity

[16] Figures 2a–2c show the averaging kernel (AK) rows for the same average of profiles observed over Delhi, India on 4 September 2004 for the TIR-only, NIR-only, and TIR + NIR retrievals. The average DFS for each retrieval type is also given. This case clearly demonstrates the advantage of a multispectral retrieval with increased sensitivity to CO near the surface as well as in the upper troposphere. Although the increase in total DFS from 1.5 to 2.0 may seem modest, by examining the TIR + NIR AK we can see significant

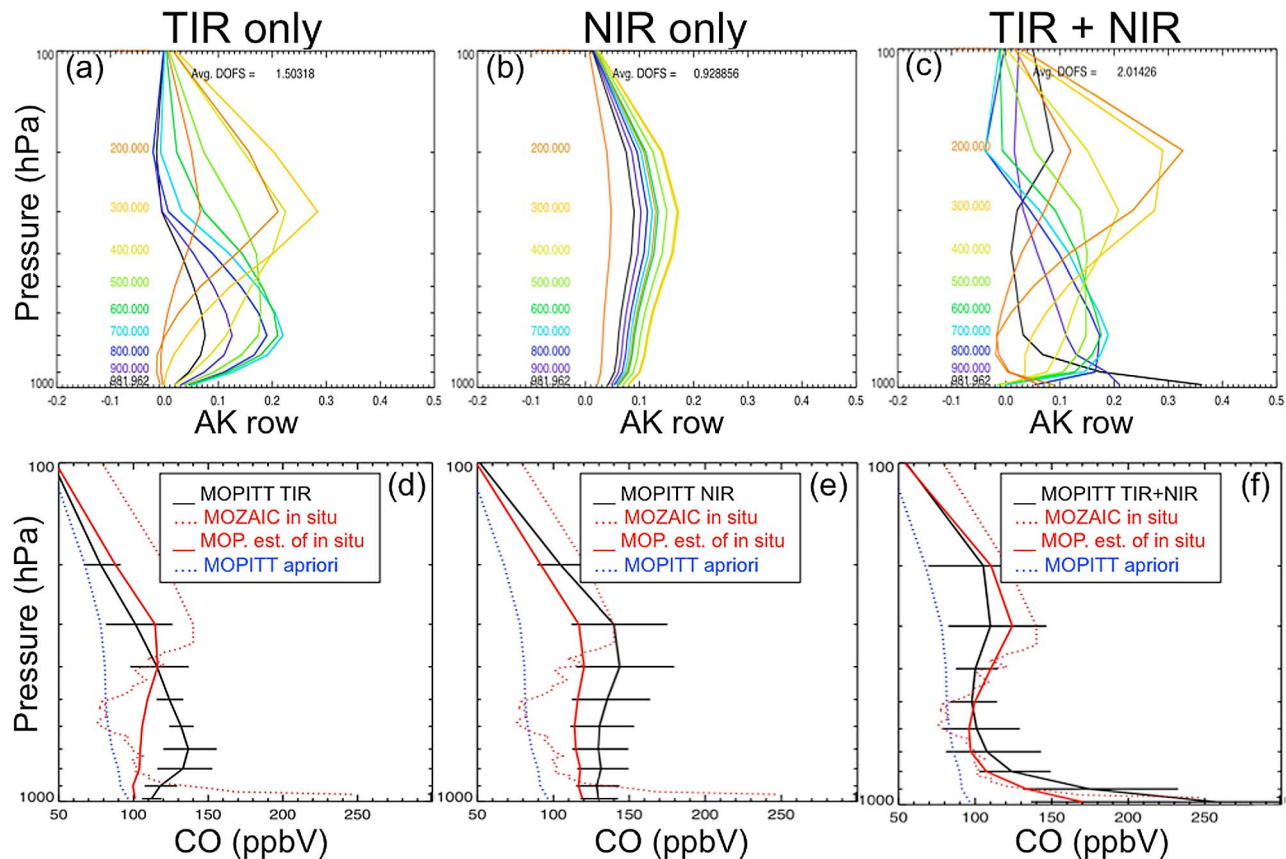


**Figure 2.** (top) Averaging kernel (AK) rows for MOPITT retrieval types (a) TIR only, (b) NIR only, and (c) multispectral TIR + NIR. (bottom) Corresponding retrieval averages (standard deviations shown as error bars) with comparisons to a MOZAIC in situ profile (augmented above  $\sim 250$  hPa using MOZART climatology) and the MOPITT estimate of the in situ profile from applying the MOPITT AK for each retrieval type and the common a priori (also shown). The same 17 profile locations are averaged in each case and were observed on 3 September 2004 within 100 km of the MOZAIC profile sampled over New Delhi, India.

improvements in the measurement ability to resolve CO in the lowermost troposphere. In particular, the AK row for the surface CO parameter is now peaked at the surface and the vertical resolution at this level improves from around 6 km for TIR-only to around 1 km for TIR + NIR. In the upper troposphere (200 hPa), the vertical resolution also improves from around 7 to 6 km. To compute the vertical resolution, we interpolate each AK row to a fine scale altitude grid (in km) and find the full-width at half maximum (FWHM). Note that this calculation is limited by the vertical spacing of the retrieval grid (100 hPa), which only allows a rough estimate.

[17] For these same retrievals we compared to an in situ profile from MOZAIC (Measurements of Ozone and Water Vapor by Airbus In-Service Aircraft) [Nedelec *et al.*, 2003]. Allowing for 100 km, 24 h coincidence, there were 17 profiles that converged for all three retrieval types. Similar to previous MOPITT validation studies [e.g., Emmons *et al.*, 2007], we follow the convention of Rodgers and Conners [2003] for applying the averaging kernel and a priori to the in situ profile in order to derive the profile that would be estimated by the MOPITT measurement and retrieval process,

$$\hat{\mathbf{x}}_{\text{MOZAIC}} = \mathbf{x}_a + \mathbf{A}[\mathbf{x}_{\text{MOZAIC}} - \mathbf{x}_a], \quad (5)$$

where  $\mathbf{x}_{\text{MOZAIC}}$  is the in situ profile from MOZAIC interpolated to the MOPITT pressure grid. In order to apply the full MOPITT AK, we augment the profile above the available MOZAIC data ( $\sim 250$  hPa) using a profile from MOZART climatology scaled to the last in situ value. Figures 2d–2f show the resulting comparisons for the retrieval types from Figures 2a–2c. The MOPITT estimate of the in situ profile, along with the average of retrieved profiles, show much better agreement with the MOZAIC profile in the TIR + NIR case. The increased standard deviations in the TIR + NIR case are due to larger random errors along with real variability in the CO profiles.

### 3. Seasonal Averages

[18] For this analysis, we have processed 5 years of MOPITT data, January 2004 to December 2008 with both TIR only and TIR + NIR retrievals, using the single a priori described above. In addition to examining total DFS and retrieved surface CO, we define the surface layer DFS as a figure of merit for evaluating lowermost troposphere sensitivity for the two retrieval types. To compute the surface layer DFS, we sum the AK diagonal elements from the

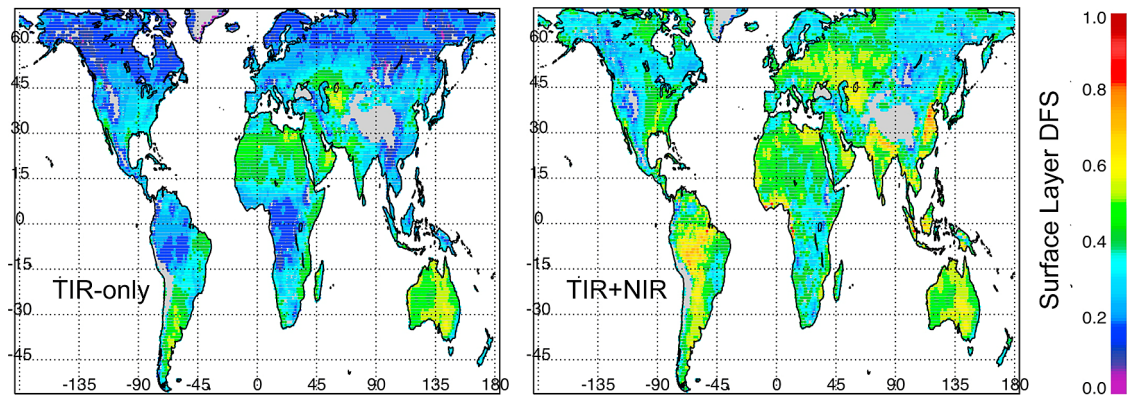


**Figure 3.** September/October/November (SON) average for 2004–2008 in  $1^\circ \times 1^\circ$  bins for the surface layer degrees of freedom for signal (DFS), defined as the trace of the averaging kernel (AK) from 800 hPa to the surface. Gray areas indicate surfaces with pressure  $< 800$  hPa. (left) TIR-only retrieval results and (right) multispectral TIR + NIR retrieval results.

surface to 800 hPa. This calculation does not apply to high altitudes with surface pressure  $< 800$  hPa, and these areas are shown in grey for Figure 3. Some of the variations seen in surface layer DFS are due to changes in the pressure depth of the lowest atmospheric layer; however, this is only significant where the topography has large variations in elevation. Values of surface layer DFS vary significantly with geography with global/annual averages of 0.25 for TIR-only cases and 0.40 for TIR + NIR cases.

### 3.1. Maps of Retrieval Sensitivity

[19] Figure 3 shows the comparison of surface layer DFS values for TIR only and TIR + NIR retrievals for the September/October/November (SON) seasonal average. Other seasons have somewhat different locations for maxima, but the SON average is representative of the common overall pattern and values. *Deeter et al.* [2007a] showed that the sensitivity to CO near the surface is highly variable in the TIR only case. The largest sensitivities in these retrievals occur in day-time land scenes with high thermal contrast between skin and air temperatures resulting from absorbed solar radiation at the surface. Scenes with moist vegetation or soil do not provide high thermal contrast due to more thermal inertia, with evapotranspiration or evaporation processes which tend to equilibrate surface and air temperatures. For NIR retrievals, sensitivity to CO is more a function of surface albedo, which can also vary significantly over different land types. As described in section 2.1, exact knowledge of the surface albedo is not necessary for the retrieval since the albedo term will cancel to first order in the radiance ratio of difference to average. However, the signal-to-noise value of  $6R$  depends on albedo since the  $6A$  term in equation (1) increases with increasing albedo. In particular, values of reflectivity for moist vegetation are  $\sim 8\%$ – $13\%$  in the  $2.3 \mu\text{m}$  range (from the ASTER database for surface reflectivity at <http://speclib.jpl.nasa.gov>), which can provide substantial NIR signals.

[20] For Figure 3, we make the general observation that areas with significant sensitivity to surface CO in the TIR-only case do not show much improvement in the combined retrieval, e.g., much of the Sahara Desert and Australia. It

appears that areas of low thermal contrast demonstrate the most significant improvements, for example, areas associated with rainforests and other vegetation, as well as some populated regions such as China. This behavior is expected after considering the separate TIR-only weighting functions and AKs [*Deeter et al.*, 2007a] and the NIR-only AKs [*Deeter et al.*, 2009]. For the TIR-only cases with high thermal contrast, there is already near-surface measurement sensitivity available and adding the total column information from the NIR will tend to be redundant at low altitudes but complementary in the upper troposphere. For moist vegetation cases with small thermal contrast, AK values for the TIR-only retrievals are close to zero at the surface. In these cases, the added information from the NIR is significant and since it is not redundant, the surface AK values in the combined TIR + NIR retrieval can be enhanced.

[21] Although the surface sensitivity for the combined retrieval is highly variable, as seen in Figure 3, we note that it is always the same or higher than the sensitivity for TIR-only retrievals. This is also true of total retrieval DFS values, shown in Figure 4, indicating that the NIR channel always adds some information in the combined TIR + NIR retrievals. The global/annual average increase in DFS is 32% for TIR-only to TIR + NIR retrievals. Statistics for each seasonal 2004–2008 average (land only, binned  $1^\circ \times 1^\circ$ ) are given in Table 1 for the increase in DFS and surface DFS, as well as the increase in percentage of cases with surface layer DFS  $> 0.4$ .

### 3.2. Maps of Estimated Surface CO

[22] Maps of the seasonal averages for MOPITT observations of surface CO are shown in Figure 5, where we have selected only those data with surface layer DFS  $> 0.4$ , which is an arbitrary threshold. The TIR-only retrievals on the left show results only over areas with high thermal contrast, as expected, while the TIR + NIR retrievals on the right have much higher coverage. The TIR + NIR maps show persistent high concentrations of CO for known source regions such as areas of biomass burning in South America, Africa, and Southeast Asia, and areas with high CO emissions from fossil fuel combustion as seen in China and the Indo-Gangetic

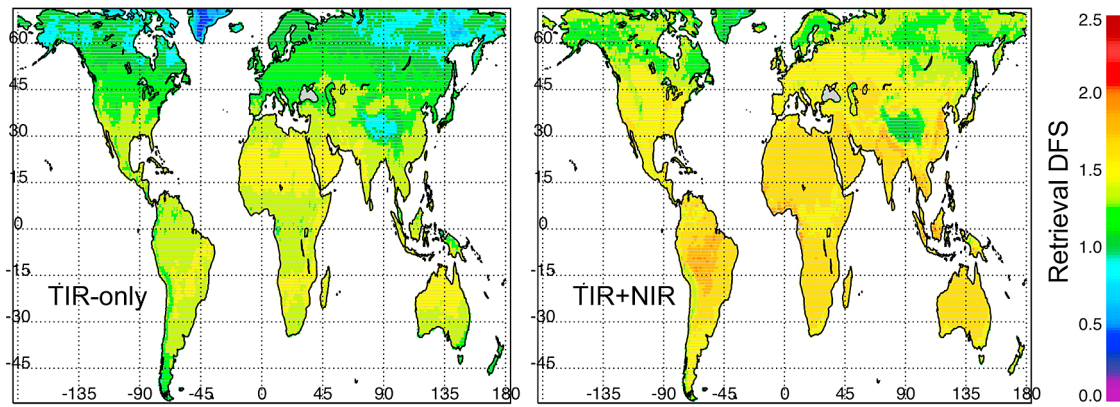


**Figure 4.** September/October/November (SON) averages for 2004–2008 in  $1^\circ \times 1^\circ$  bins for the degrees of freedom for signal (DFS). (left) TIR-only retrieval results and (right) multispectral TIR + NIR retrieval results.

plane [Edwards *et al.*, 2006; Clerbaux *et al.*, 2008]. Seasonal variations in CO distributions depend on local CO sources and on solar radiation since this is a primary factor controlling hydroxyl (OH) concentrations, the main chemical sink for CO [Holloway *et al.*, 2000]. In Figure 5, we see expected seasonal CO variations with high latitude late winter/early spring maxima due to less chemical destruction by OH and tropical distributions corresponding to known biomass burning patterns [Giglio *et al.*, 2006].

#### 4. Improved Sensitivity to Surface CO in China

[23] With a rapidly expanding economy and several high-density population centers, China now leads the world in emissions from fossil fuel burning, primarily from an increase in coal use [Boden *et al.*, 2009; Gregg *et al.*, 2008; Tie *et al.*, 2006], but also from a growing number of vehicles [Cai and Xie, 2007]. Clerbaux *et al.* [2008] show how CO emission inventories and a long-term (7.5 year) average of CO mixing ratio observations from MOPITT correspond to areas of high population density in China. This study and others, such as Buchwitz *et al.* [2007] using SCIAMACHY CO column data, NO<sub>2</sub> observations from Richter *et al.* [2005], and multisatellite observations of improved air quality during the 2008 Olympics in Beijing [Witte *et al.*, 2009] have demonstrated the ability to observe regional pollution distributions over China from space.

[24] In Figure 6, we show significant improvements in MOPITT sensitivity to surface CO in China. This shows the comparison of TIR-only versus TIR + NIR retrievals of surface CO for the September–October–November (SON) seasonal average over  $75^\circ\text{E}–135^\circ\text{E}$ ,  $10^\circ\text{N}–40^\circ\text{N}$ . Compared to TIR-only, the TIR + NIR retrievals show clear patterns of surface CO corresponding to high density population areas in Central/East Asia. For this plot, we did not filter with a surface layer DFS threshold. For the TIR-only case, the surface DFS values vary from 0 to 0.4 so that most areas have surface CO near the a priori values, (e.g., 100 ppbv at 1000 hPa). In the TIR + NIR case, most of this region had high sensitivity, e.g., surface layer DFS > 0.5 (except the Tibetan plateau). Although the TIR + NIR surface CO VMRs are high near the urban areas, the retrieved values are affected by both vertical smoothing and the a priori and will still tend to be lower than in situ surface measurements. For example, from the MOZAIC data used in the comparisons for this paper, the Shanghai area has surface CO values up to 650 ppbv. Although using a common, static a priori clearly demonstrates the differences due only to adding the NIR channels, with a realistic a priori, we could obtain more accurate surface CO values. Multispectral retrievals with a variable climatological a priori would better compare with surface in situ measurements since sensitivity to the surface is enhanced, but still not perfect. TIR + NIR retrievals with the MOPITT V4 variable a priori will be tested in future work, however, since the a priori and AK are provided with

**Table 1.** Seasonal Average Statistics for Differences Between TIR + NIR and TIR-Only Retrievals for DFS and Surface Layer DFS Values<sup>a</sup>

Season	Average $\Delta\text{DFS}$	Std. Dev. $\Delta\text{DFS}$	Max. $\Delta\text{DFS}$	Average $\Delta\text{DFS}_{\text{srf}}$	Std. Dev. $\Delta\text{DFS}_{\text{srf}}$	%TIR-only $\text{srfDFS}>0.4$	%TIR + NIR $\text{srfDFS}>0.4$
DJF	0.41	0.20	1.18	0.19	0.13	9.0	37.1
MAM	0.35	0.18	0.92	0.13	0.10	15.0	35.3
JJA	0.25	0.09	1.10	0.11	0.09	16.8	52.8
SON	0.35	0.17	0.95	0.15	0.11	12.8	36.7
Annual average (all latitudes)						13.2	39.8
Annual average (tropics: $23.4^\circ\text{S}–23.4^\circ\text{N}$ )						19.7	59.0

<sup>a</sup> $\Delta\text{DFS} = \text{DFS}_{\text{TIR+NIR}} - \text{DFS}_{\text{TIR-only}}$  and  $\Delta\text{DFS}_{\text{srf}} = \text{srfDFS}_{\text{TIR+NIR}} - \text{srfDFS}_{\text{TIR-only}}$ . Also given are the percentage of retrievals with surface layer DFS values at least 0.4.

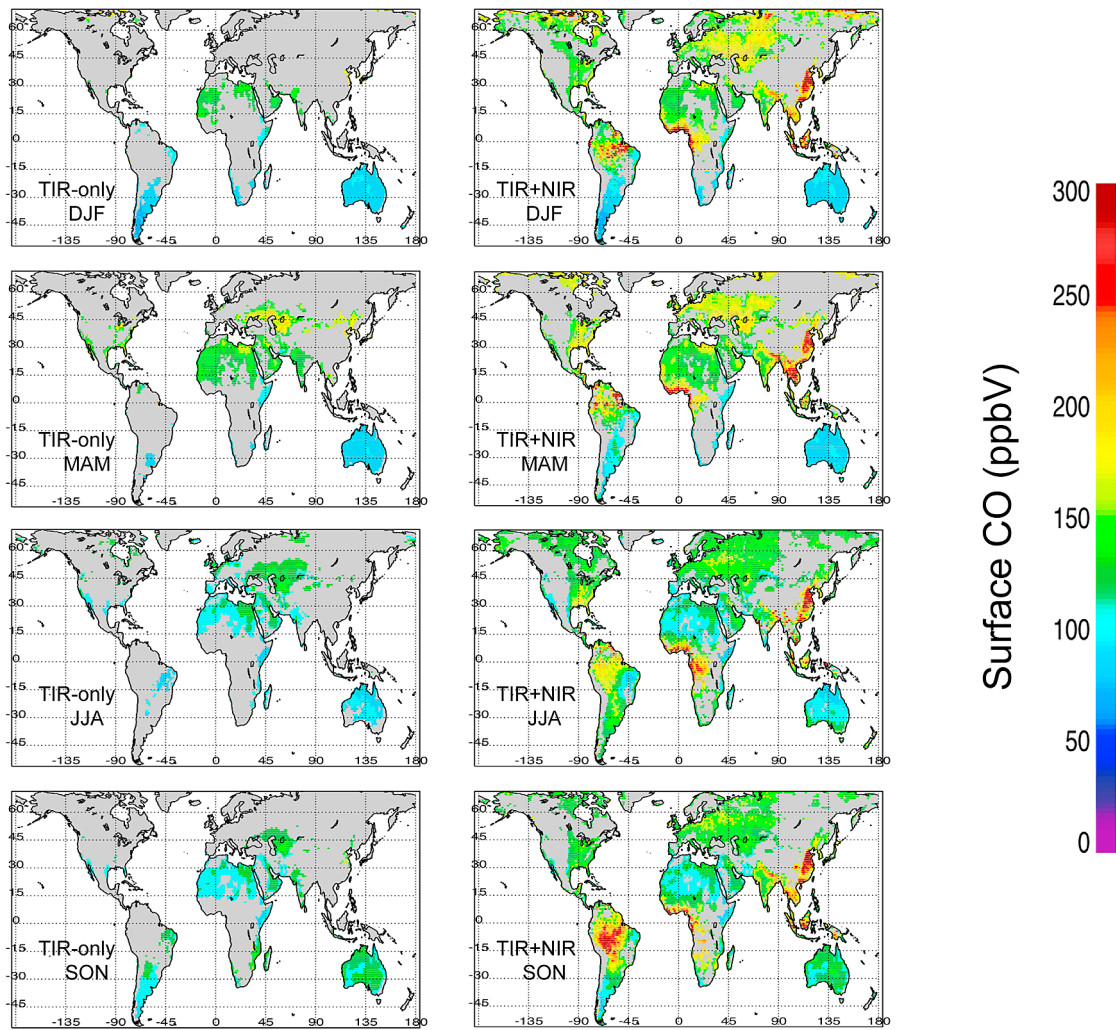


**Figure 5.** Surface CO mixing ratios for seasonal averages, 2004–2008, where we have selected only those data with surface layer DFS > 0.4. (left) TIR-only retrieval results and (right) multispectral TIR + NIR retrieval results. Gray areas indicate surface layer DFS below the threshold (which includes surfaces with pressure < 800 hPa).

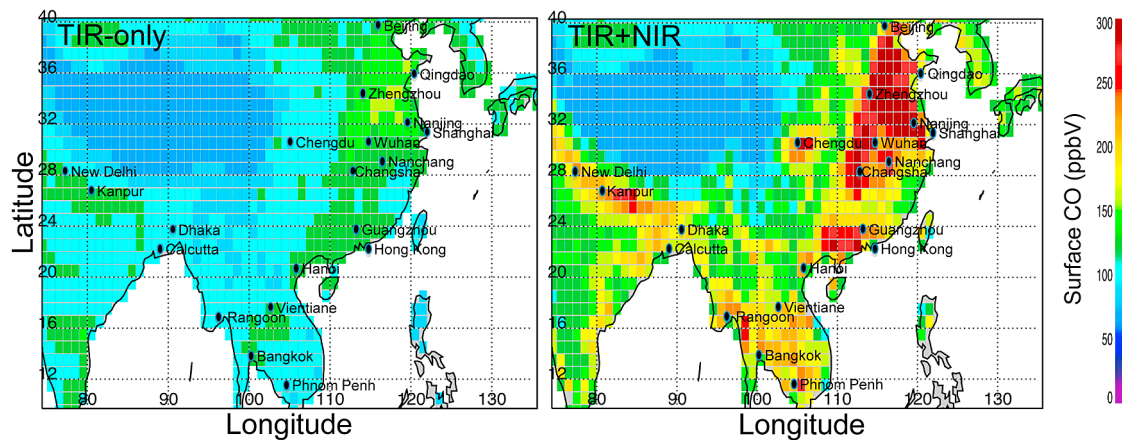


**Figure 6.** Surface CO seasonal averages for 2004–2008, September/October/November (SON) in Central/East Asia. (left) TIR-only retrieval results and (right) multispectral TIR + NIR retrieval results.

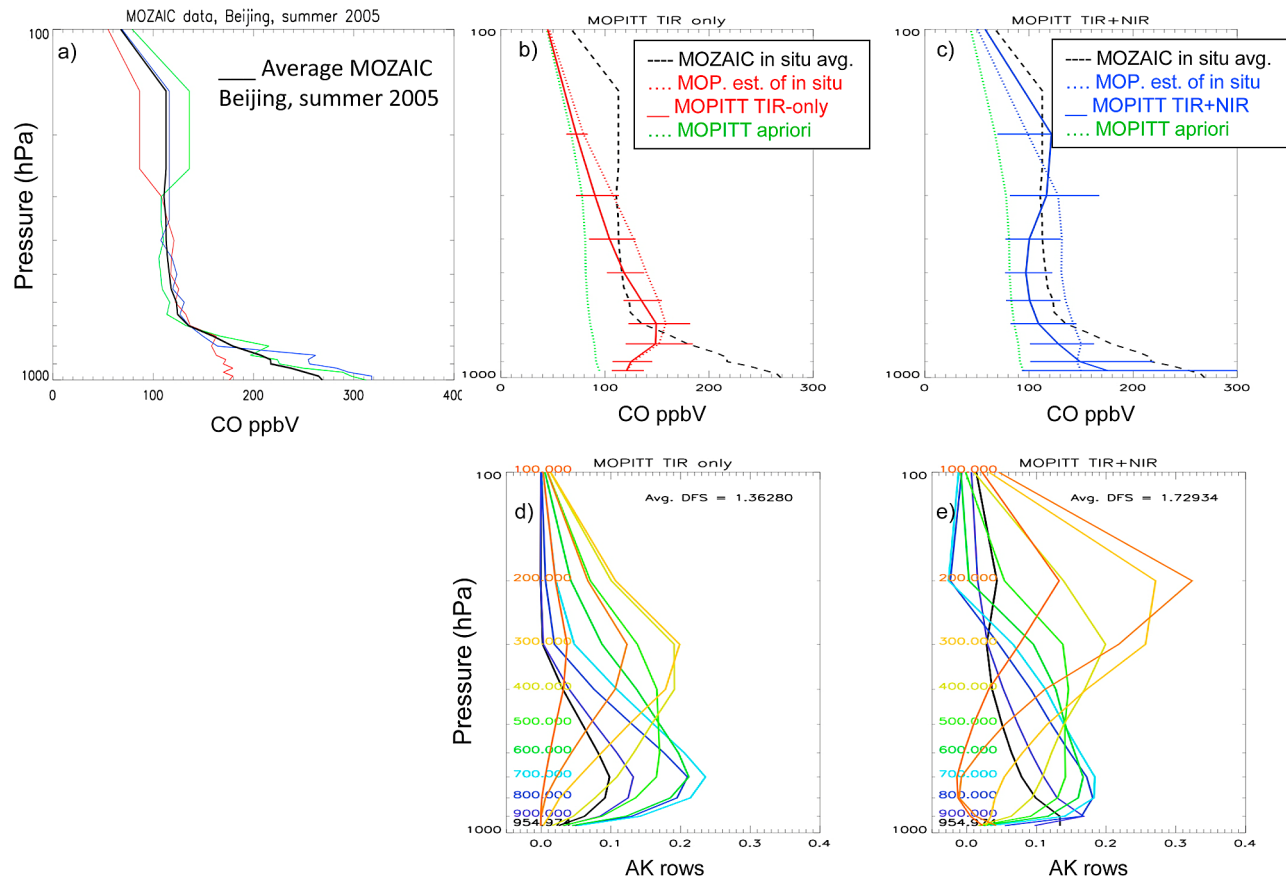


**Figure 7.** MOZAIC data and comparisons with MOPITT retrievals for Beijing, summer 2005. (a) The individual MOZAIC profiles (augmented above  $\sim 250$  hPa using MOZART climatology) in different colors and the average MOZAIC profile in black. (b) TIR-only and (c) TIR + NIR show retrieval averages (standard deviations shown as error bars) with comparisons to the average MOZAIC in situ profile and the MOPITT estimate of the in situ profile from applying the MOPITT AK for each retrieval type and the common a priori (also shown). (d) TIR-only and (e) TIR + NIR show the corresponding AK row averages. Profiles and AKs are averages of 41 MOPITT observations with 4 h, 100 km coincidence of three MOZAIC profiles sampled over Beijing. Comparison dates are 15 June 2005 and 2 August 2005 (two MOZAIC profiles).

each retrieval, a static, global a priori can be substituted, if needed, to make the comparisons as shown here.

[25] We note that the previous study by Clerbaux *et al.* [2008] analyzed MOPITT V3 (TIR-only) data, which used an a priori covariance error with a larger effective correlation distance than used for MOPITT V4 data [Deeter *et al.*, 2010], or for this study. Because of the larger correlation distance, the CO values at the surface in the V3 retrievals were strongly influenced by free tropospheric retrieval levels where MOPITT sensitivity is much higher in the TIR-only case. The smaller correlation distance used in the retrievals for this study explains why the TIR-only result for surface CO shown here, which displays only weak enhancements over China, is different from the Clerbaux *et al.* [2008] MOPITT V3 result.

[26] To provide an initial evaluation of these retrievals, we use MOZAIC profiles from Beijing and Shanghai shown in Figures 7 and 8, respectively. These figures show averaged profiles for 4 h, 100 km coincidence with

MOZAIC data, where both TIR-only and TIR + NIR MOPITT estimates were available. For these averages, we selected observations where adding the NIR channel provided an increase in DFS. In the cases where the NIR channel does not increase sensitivity, the retrievals are identical to the TIR-only retrievals. As in Figure 2, the MOPITT estimates of the in situ profiles, along with the averages of retrieved profiles, are in much better agreement with the MOZAIC data in the TIR + NIR cases compared to the TIR-only cases, for both the values near the surface and the overall profile shape. However, in both cities, we fall short of estimating the CO VMR values at the surface measured by MOZAIC. Some of the difference is to be expected given the a priori and AK values; however, there is always a potential difference caused by the spatial representativeness of the MOPITT footprint (22 km) compared to the in situ profile, even with close coincidence criteria for the comparison. As suggested above, with a more realistic a priori, MOPITT multispectral retrievals

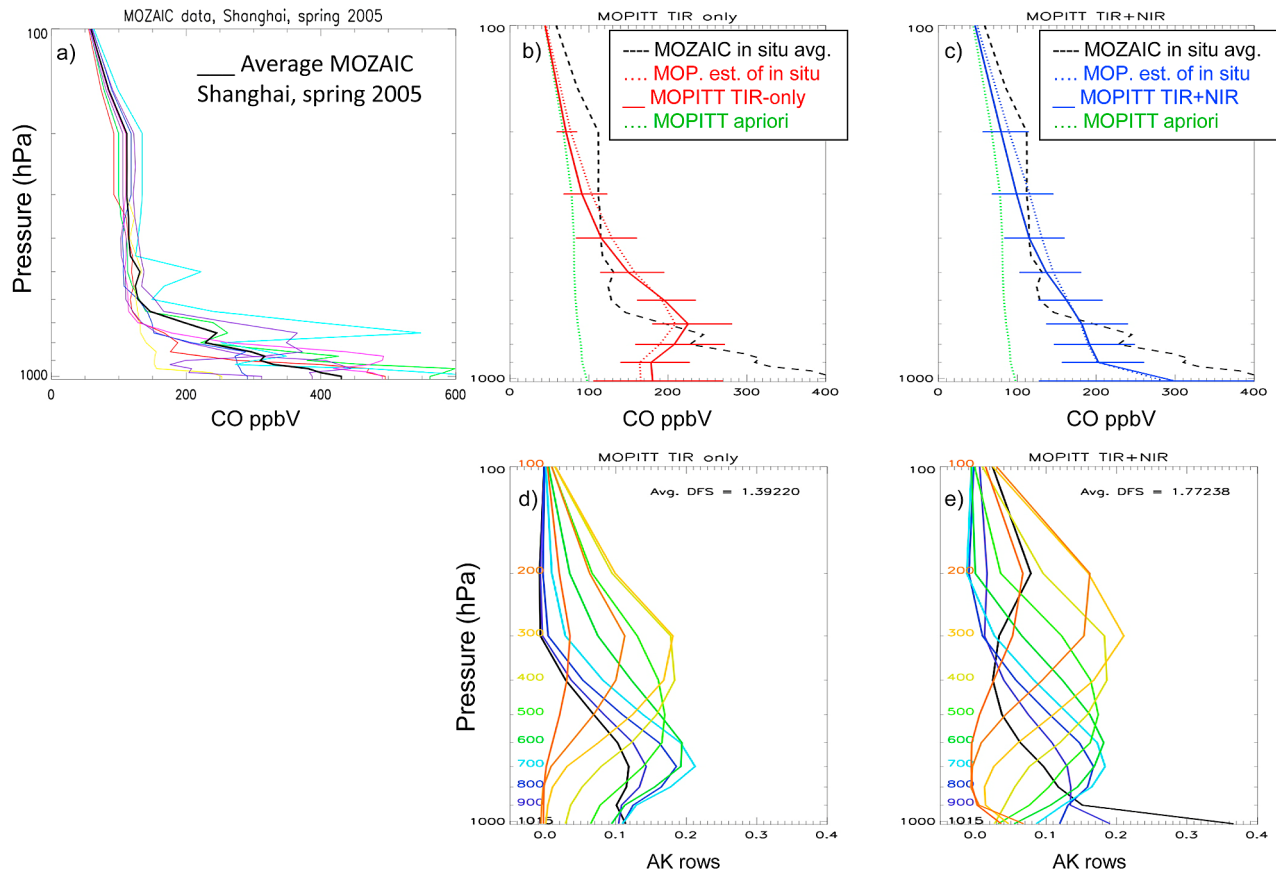


**Figure 8.** Same as Figure 7 but for Shanghai, spring 2005. Profiles and AKs are averages of 75 MOPITT observations with 4 h, 100 km coincidence of 8 MOZAIC profiles sampled over Shanghai. Comparison dates are 15, 17, 24, and 31 March 2005 and 2, 7 (two MOZAIC profiles), and 16 April 2005.

with surface layer sensitivity should be closer to the in situ measurements, but more precise comparisons would still be limited by MOPITT horizontal resolution and improvements to this will have to await new satellite instruments.

## 5. Conclusions

[27] By analyzing the retrieval degrees of freedom for signal (DFS) for the surface to 800 hPa, we have demonstrated the increased sensitivity of MOPITT multispectral retrievals to CO in the lowest part of the atmosphere. Seasonal averages on global and continental scales illustrate the improvements in surface CO estimates. Since we have used a single a priori in all the retrievals, we show that the relative increase in estimated surface CO is due only to applying a multispectral (TIR + NIR) retrieval as compared to a TIR-only retrieval.

[28] Future MOPITT data products will include TIR + NIR retrievals while retaining the TIR-only capability for night and ocean coverage. Work to better characterize the geophysical variability in the NIR measurements is ongoing and should result in a scene-dependent noise value for future retrievals. This would be more accurate than the single value for geophysical noise assumed for this study and would allow better filtering based on individual scene

quality. Results presented in this paper achieve increased sensitivity to CO by effectively underestimating the radiance error covariance matrix. This is equivalent to the suboptimal estimation method described by equation (4.52) of Rodgers [2000], which will be applied to derive a more realistic a posteriori covariance matrix in future studies. Analysis to quantify errors due to aerosol contamination will also be performed. The improved representation of errors along with more extensive validation with surface and aircraft CO measurements and scientific evaluation using models will be topics of future publications.

[29] Currently available TIR-only and NIR-only data provide very limited information about near-surface CO. Although the MOPITT multispectral retrievals do not have sensitivity to the lowermost troposphere everywhere, they represent a significant increase in measurement capability. When properly exploited with the AK to account for information from the measurement versus the a priori, these multispectral CO data should provide a direct constraint for the transport of CO from source regions into the troposphere. This will add significant information about the lowest layer of the atmosphere in data assimilation and should allow improved emissions estimates. Since MOPITT data spans over 10 years, the multispectral retrievals will provide a new perspective on the evolution of CO sources

over the past decade. This demonstration of the MOPITT multispectral capability is also very relevant to future satellite missions, especially for carbon-cycle and air quality applications.

### Acronyms

AIRS	Atmospheric Infrared Sounder
AK	Averaging Kernel
AOD	aerosol optical depth
DFS	Degrees of Freedom for Signal
DJF	December/January/February
EOS	Earth Observing System
hPa	hecto-Pascal
IASI	Infrared Atmospheric Sounding Interferometer
JJA	June/July/August
LMC	length modulated cell
MAM	March/April/May
MODIS	Moderate-Resolution Imaging Spectroradiometer
MOPITT	Measurement of Pollution in the Troposphere
MOZAIC	Measurements of Ozone and Water Vapor by Airbus In-Service Aircraft
NIR	near infrared
OSSE	Observation System Simulation Experiment
PMC	pressure modulated cell
ppp	parts per billion
SCIAMACHY	Scanning Imaging Absorption Spectrometer for Atmospheric Chartography
SON	September/October/November
TES	tropospheric emission spectrometer
TIR	thermal infrared
TOA	top of atmosphere
UV	ultraviolet
VMR	volume mixing ratio

[30] **Acknowledgments.** The authors thank Gene Francis, Dallas Masters, and Debbie Mao at National Center for Atmospheric Research (NCAR) for their support in algorithms and data processing, and we appreciate the helpful comments from Gabriele Pfister and Liwen Pan. The MOPITT team also acknowledges the contributions of COMDEV (the prime contractor) and ABB BOMEM with support from the Canadian Space Agency (CSA), the Natural Sciences and Engineering Research Council (NSERC), and Environment Canada. The authors acknowledge for their strong support the European Communities, EADS, Airbus, and the airlines (Lufthansa, Austrian, Air France) who carry free of charge the MOZAIC equipment and perform the maintenance since 1994. MOZAIC is presently funded by INSU-CNRS (France), Météo-France, and Forschungszentrum (FZJ, Juelich, Germany). The MOZAIC database is supported by ETHER (CNES and INSU-CNRS). The NCAR MOPITT project is supported by the National Aeronautics and Space Administration (NASA) Earth Observing System (EOS) Program. The National Center for Atmospheric Research (NCAR) is sponsored by the National Science Foundation.

### References

Ackerman, S. A., K. I. Strabala, W. P. Menzel, R. A. Frey, C. C. Moeller, and L. E. Gumley (1998), Discriminating clear sky from clouds with MODIS, *J. Geophys. Res.*, *103*(D24), 32,141–32,157, doi:10.1029/1998JD200032.

Arellano, A. F., P. S. Kasibhatla, L. Giglio, G. R. van der Werf, and J. T. Randerson (2004), Top-down estimates of global CO sources using MOPITT measurements, *Geophys. Res. Lett.*, *31*, L01104, doi:10.1029/2003GL018609.

Boden, T. A., G. Marland, and R. J. Andres (2009), Global, Regional, and National Fossil-Fuel CO<sub>2</sub> Emissions. Carbon Dioxide Information Analysis Center, Oak Ridge Natl. Lab., U.S. Dep. of Energy, Oak

Ridge, Tenn., doi:10.3334/CDIAC/00001. (Available at <http://cdiac.ornl.gov/trends/emis/cpa.html>)

Buchwitz, M., R. de Beek, K. Bramstedt, S. Noël, H. Bovensmann, and J. P. Burrows (2004), Global carbon monoxide as retrieved from SCIAMACHY by WFM-DOAS, *Atmos. Chem. Phys.*, *4*, 1945–1960.

Buchwitz, M., I. Khlystova, H. Bovensmann, and J. P. Burrows (2007), Three years of global carbon monoxide from SCIAMACHY: Comparison with MOPITT and first results related to the detection of enhanced CO over cities, *Atmos. Chem. Phys.*, *7*, 2399–2411.

Cai, H., and S. Xie (2007), Estimation of vehicular emission inventories in China from 1980 to 2005, *Atmos. Environ.*, *44*(39), 8963.

Christi, M., and G. Stephens (2004), Retrieving profiles of atmospheric CO<sub>2</sub> in clear sky and in the presence of thin cloud using spectroscopy from the near and thermal infrared: A preliminary case study, *J. Geophys. Res.*, *109*, D04316, doi:10.1029/2003JD004058.

Clerbaux, C., D. P. Edwards, M. Deeter, L. Emmons, J.-F. Lamarque, X. X. Tie, S. T. Massie, and J. Gille (2008), Carbon monoxide pollution from cities and urban areas observed by the Terra/MOPITT mission, *Geophys. Res. Lett.*, *35*, L03817, doi:10.1029/2007GL032300.

Deeter, M. N., et al. (2003), Operational carbon monoxide retrieval algorithm and selected results for the MOPITT instrument, *J. Geophys. Res.*, *108*(D14), 4399, doi:10.1029/2002JD003186.

Deeter, M. N., L. K. Emmons, D. P. Edwards, J. C. Gille, and J. R. Drummond (2004), Vertical resolution and information content of CO profiles retrieved by MOPITT, *Geophys. Res. Lett.*, *31*, L15112, doi:10.1029/2004GL020235.

Deeter, M. N., D. P. Edwards, J. C. Gille, and J. R. Drummond (2007a), Sensitivity of MOPITT observations to carbon monoxide in the lower troposphere, *J. Geophys. Res.*, *112*, D24306, doi:10.1029/2007JD008929.

Deeter, M. N., D. P. Edwards, and J. C. Gille (2007b), Retrievals of carbon monoxide profiles from MOPITT observations using lognormal a priori statistics, *J. Geophys. Res.*, *112*, D11311, doi:10.1029/2006JD007999.

Deeter, M. N., D. P. Edwards, J. C. Gille, and J. R. Drummond (2009), CO retrievals based on MOPITT near-infrared observations, *J. Geophys. Res.*, *114*, D04303, doi:10.1029/2008JD010872.

Deeter, M. N., et al. (2010), The MOPITT version 4 CO product: Algorithm enhancements, validation, and long-term stability, *J. Geophys. Res.*, *115*, D07306, doi:10.1029/2009JD013005.

Drummond, J. R. (1992), Measurements of pollution in the troposphere (MOPITT), in *The Use of EOS for Studies of Atmospheric Physics*, edited by J. C. Gille and G. Visconti, pp. 77–101, North-Holland, New York.

Drummond, J. R., J. Zou, F. Nichitiu, J. Kar, R. Deschambaut, and J. Hackett (2009), A review of 9-year performance and operation of the MOPITT instrument, *J. Adv. Space Res.*, *45*, 760–774, doi:10.1016/j.asr.2009.11.019.

Edwards, D., C. Halvorson, and J. Gille (1999), Radiative transfer modeling for the EOS Terra satellite measurement of pollution in the troposphere (MOPITT) instrument, *J. Geophys. Res.*, *104*(D14), 16,755–16,775, doi:10.1029/1999JD900167.

Edwards, D. P., et al. (2006), Satellite-observed pollution from Southern Hemisphere biomass burning, *J. Geophys. Res.*, *111*, D14312, doi:10.1029/2005JD006655.

Edwards, D. P., A. F. Arellano, and M. N. Deeter (2009), A satellite observation system simulation experiment for carbon monoxide in the lowermost troposphere, *J. Geophys. Res.*, *114*, D14304, doi:10.1029/2008JD011375.

Emmons, L. K., G. G. Pfister, D. P. Edwards, J. C. Gille, G. Sachse, D. Blake, S. Wofsy, C. Gerbig, D. Matross, and P. Nédélec (2007), Measurements of pollution in the troposphere (MOPITT) validation exercises during summer 2004 field campaigns over North America, *J. Geophys. Res.*, *112*, D12S02, doi:10.1029/2006JD007833.

George, M., et al. (2009), Carbon monoxide distributions from the IASI/METOP mission: evaluation with other space-borne remote sensors, *Atmos. Chem. Phys.*, *9*, 8317–8330.

Giglio, L., I. Csizsar, and C. O. Justice (2006), Global distribution and seasonality of active fires as observed with the Terra and Aqua Moderate Resolution Imaging Spectroradiometer (MODIS) sensors, *J. Geophys. Res.*, *111*, G02016, doi:10.1029/2005JG000142.

Gloudemans, A. M. S., H. Schrijver, O. P. Hasekamp, and I. Aben (2008), Error analysis for CO and CH<sub>4</sub> total column retrievals from SCIAMACHY 2.3 μm spectra, *Atmos. Chem. Phys.*, *8*, 3999–4017.

Gregg, J. S., R. J. Andres, and G. Marland (2008), China: Emissions pattern of the world leader in CO<sub>2</sub> emissions from fossil fuel consumption and cement production, *Geophys. Res. Lett.*, *35*, L08806, doi:10.1029/2007GL032887.

Holloway, T., H. Levy II, and P. Kasibhatla (2000), Global distribution of carbon monoxide, *J. Geophys. Res.*, *105*(D10), 12,123–12,147, doi:10.1029/1999JD901173.

- Jones, D. B. A., K. W. Bowman, J. A. Logan, C. L. Heald, J. Liu, M. Luo, J. Worden, and J. Drummond (2009), The zonal structure of tropical O<sub>3</sub> and CO as observed by the Tropospheric Emission Spectrometer in November 2004: Part 1. Inverse modeling of CO emissions, *Atmos. Chem. Phys.*, *9*, 3547–3562.
- Kopacz, M., et al. (2010), Global estimates of CO sources with high resolution by adjoint inversion of multiple satellite datasets (MOPITT, AIRS, SCIAMACHY, TES), *Atmos. Chem. Phys.*, *10*, 855–876.
- Landgraf, J., and O. P. Hasekamp (2007), Retrieval of tropospheric ozone: The synergistic use of thermal infrared emission and ultraviolet reflectivity measurements from space, *J. Geophys. Res.*, *112*, D08310, doi:10.1029/2006JD008097.
- Luo, M., et al. (2007), Comparison of carbon monoxide measurements by TES and MOPITT: The influence of a priori data and instrument characteristics on nadir atmospheric species retrievals, *J. Geophys. Res.*, *112*, D09303, doi:10.1029/2006JD007663.
- Nedelec, P., J.-P. Cammas, V. Thouret, G. Athier, J.-M. Cousin, C. Legrand, C. Abonneil, F. Lecoour, G. Cayez, and C. Marizy (2003), An improved infrared carbon monoxide analyser for routine measurements aboard commercial Airbus aircraft: technical validation and first scientific results of the MOZAIC III programme, *Atmos. Chem. Phys.*, *3*, 1551–1564.
- Pan, L. W., D. P. Edwards, J. C. Gille, M. W. Smith, and J. R. Drummond (1995), Satellite remote-sensing of tropospheric CO and CH<sub>4</sub> – forward model studies of the MOPITT instrument, *Appl. Optics*, *34*, 6976–6988.
- Pan, L. W., J. C. Gille, D. P. Edwards, P. L. Bailey, and C. D. Rodgers (1998), Retrieval of tropospheric carbon monoxide for the MOPITT experiment, *J. Geophys. Res.*, *103*, 32,277–32,290.
- Pfister, G., P. G. Hess, L. K. Emmons, J.-F. Lamarque, C. Wiedinmyer, D. P. Edwards, G. Pétron, J. C. Gille, and G. W. Sachse (2005a), Quantifying CO emissions from the 2004 Alaskan wildfires using MOPITT CO data, *Geophys. Res. Lett.*, *32*, L11809, doi:10.1029/2005GL022995.
- Pfister, G., J. C. Gille, D. Ziskin, G. Francis, D. P. Edwards, and M. N. Deeter (2005b) Effects of a spectral surface reflectance on measurements of backscattered solar radiation: Application to the MOPITT methane retrieval, *J. Atmos. Oceanic Technol.*, *22*, 566–574.
- Razavi, A., C. Clerbaux, C. Wespes, L. Clarisse, D. Hurtmans, S. Payan, C. Camy-Peyret, and P. F. Coheur (2009), Characterization of methane retrievals from the IASI space-borne sounder, *Atmos. Chem. Phys.*, *9*, 7889–7899.
- Richter, A., P. Burrows, H. Nues, C. Granier, and U. Niemeijer (2005), Increase in tropospheric nitrogen dioxide over China observed from space, *Nature*, *437*, 129–130.
- Rodgers, C. (2000), *Inverse Methods for Atmospheric Sounding: Theory and Practice*, World Sci., London.
- Rodgers, C., and B. Conners (2003), Intercomparison of remote sounding instruments, *J. Geophys. Res.*, *108*(D3), 4116, doi:10.1029/2002JD002299.
- Tie, X., et al. (2006), Chemical characterization of air pollution in eastern China and the eastern United States, *Atmos. Environ.*, *40*, 2607–2625.
- Tolton, B. T., and J. R. Drummond (1997), Characterization of the length-modulated radiometer, *Appl. Opt.*, *36*, 5409–5419.
- Turquet, S., et al. (2008), CO emission and export from Asia: An analysis combining complementary satellite measurements (MOPITT, SCIAMACHY and ACE-FTS) with global modeling, *Atmos. Chem. Phys.*, *8*, 5187–5204.
- Warner, J. X., J. C. Gille, D. P. Edwards, D. C. Ziskin, M. W. Smith, P. L. Bailey, and L. Rokke (2001), Cloud detection and clearing for the Earth Observing System Terra satellite Measurements of Pollution in the Troposphere (MOPITT) experiment, *Appl. Opt.*, *40*, 1269–1284.
- Warner, J. X., M. McCourt Comer, C. Barnet, W. W. McMillan, W. Wolf, E. Maddy, and G. Sachse (2007), A comparison of satellite tropospheric carbon monoxide measurements from AIRS and MOPITT during INTEX-NA, *J. Geophys. Res.*, *112*, D12S17, doi:10.1029/2006JD007925.
- Witte, J. C., M. R. Schoeberl, A. R. Douglass, J. F. Gleason, N. A. Krotkov, J. C. Gille, K. E. Pickering, and N. Livesey (2009), Satellite observations of changes in air quality during the 2008 Beijing Olympics and Paralympics, *Geophys. Res. Lett.*, *36*, L17803, doi:10.1029/2009GL039236.
- Worden, J., X. Liu, K. Bowman, K. Chance, R. Beer, A. Eldering, M. Gunson, and H. Worden (2007), Improved Tropospheric Ozone Profile Retrievals Using OMI and TES Radiances, *Geophys. Res. Lett.*, *34*, L01809, doi:10.1029/2006GL027806.

M. N. Deeter, D. P. Edwards, J. C. Gille, and H. M. Worden, Atmospheric Chemistry Division, National Center for Atmospheric Research, Boulder, CO 80307, USA. (hmw@ucar.edu)

J. R. Drummond, Department of Physics and Atmospheric Science, Dalhousie University, Halifax, NS B3H 3J5, Canada.

P. Nédélec, Laboratoire d'Aérodologie, University P. Sabatier, Centre National de la Recherche Scientifique, Observatoire Midi-Pyrénées, F-31400 Toulouse, France.